Modified Graphite with Tin Oxide as a Promising Electrode for Reduction of Organic Pollutants from Wastewater by Sonoelectrochemical Oxidation

Hind Jabbar Nsaif[1*], Najwa Saber Majeed[1]

[1] Department of Chemical Engineering, College of Engineering, University of Baghdad, Baghdad, Iraq
* Corresponding author's e-mail: hind.nsaif1507d@coeng.uobaghdad.edu.iq

ABSTRACT

Most of the studies on tin oxide coatings as electrode materials were conducted on titanium; in this study, the aim was to create pure tin oxide (SnO_2) films on graphite substrate, which is more prevalent than titanium. There is a lack in investigation the effect of $SnCl_2$ and HNO_3 concentrations on the prepared SnO_2 electrode; therefore, the aim of this work was to study these effects precisely. Also, no previous study investigated the removal of phenol sonoelectrochemically by a SnO_2 electrode, which would be accomplished in the present work. The tin dioxide electrode was produced by cathodic electrodeposition using a $SnCl_2 \cdot 2H_2O$ solution in the presence of HNO_3 and $NaNO_3$ on a graphite plate substrate. The impact of various operating parameters (current density – CD, HNO_3 concentration, and $SnCl_2 \cdot 2H_2O$ concentration) on the morphology and structure of the SnO_2 deposit layer was thoroughly investigated. The physical structures of the SnO_2 film were determined by X-ray diffraction (XRD), surface morphology was characterized using field-emission scanning electron microscopy (SEM), and chemical composition was analyzed using energy-dispersive X-ray spectroscopy (EDX). In a batch reactor, the sonoelectrochemical oxidation of phenol was tested to determine the performance of the best SnO_2 electrodes for phenol degradation and any organic byproducts. It was discovered that 10 mA/cm², 50 mM of $SnCL_2 \cdot 2H_2O$, and 250 mM of HNO_3 were the optimum conditions to prepare SnO_2 electrodes, which produced the smallest crystal size, with no appeared cracks, and gave the best phenol removal. The best prepared electrode was tested in the sonoelectrochemical oxidation of phenol with two different electrolytes and different CD, and the results showed that the phenol removal was 76.87% and 64.68% when using NaCl and Na_2SO_4, respectively, as well as was 63.39, 76.87, and 100% for CD at 10, 25, and 40 mA/cm², respectively.

Keywords: tin dioxide, electrodeposition, sonoelectrochemical, phenol removal.

INTRODUCTION

There is a serious issue with increased demand and a shortage of clean water supplies on a global scale because of faster industrial expansion, population growth, and extended droughts. Large-scale environmental pollution from industrial wastewater discharges necessitates the creation and implementation of effective treatment methods that can eliminate the dangerous contaminants present in these industrial streams (Al-Alawy et al., 2017). Water is used in vast amounts throughout the refining process in the petroleum

industry (Dhamin et al., 2022) According to a survey, the amount of wastewater produced by the methods used to refine oil is 1.6 times greater than the total amount of crude oil treated, and between 80 and 90% of the water used in the process (Majeed, 2017). The compounds contained in contaminated water are diverse and complicated, including chemical oxygen demand (COD), varied amounts of emulsified oil, heavy metals, organic compounds, aromatic hydrocarbons, oils and greases, phenol, and occasionally radioactive elements. Phenol and its derivatives are the most prevalent organic contaminants found in

oil refining industry wastewaters. Because of their high toxicity, limited biodegradability, and ecological impact, these substances are particularly dangerous (Naser et al., 2021). Phenolic compounds are very dangerous for the environment because of their severe toxicity, even at extremely low concentrations (Al-Jandeel, 2013), stability, bioaccumulation, and low biodegradability. Phenolic compounds hurt human health both immediately and over time (Al-Obaidy, 2013; Mezaal, 2019).

Wastewater is treated using several methods, including coagulation, adsorption, oxidation, biological processing, and electrochemical processes (Thwaini et al., 2023). Conventional treatment methods only transfer pollutants from one medium to another while producing secondary waste and typically consume a lot of energy (Kassob et al., 2022; Fajri et al., 2023). Due to the difficulties in using conventional wastewater treatment techniques, combining ultrasound and electrochemistry, which is called sonelectrochemistry, may be a viable choice (Ang et al., 2022). There are several advantages of sonoelectrochemistry, like chemical and physical influence of ultrasound that generate oxidizing species like OH$\cdot$ radicals and H_2O_2, disturbance of the diffusion layer, enhanced ion mass transfer over the double layer, as well as periodic cleaning and reactivation of the electrode surfaces. All of these impacts work together to increase yield and enhance electrical efficiency, so sonoelectrochemistry is promising for the removal of organic pollutants (Thokchom et al., 2015).

The efficiency of sonoelectrochemistry is significantly influenced by the electrode materials. The electrodes must undergo a high oxygen evolution reaction (OER) to generate a significant amount of OH$\cdot$ radicals, which is advantageous for the oxidation of organic pollutants on the electrode surface. Boron-doped diamond (BDD), Ti/PbO_2, and Ti/SnO_2 electrodes all have quite high OER potential (Zhao et al., 2015). PbO_2 electrodes are thought to have adequate electrocatalytic capability for oxidizing organic compounds. However, the concerns about the potential toxicity of Pb leaking from the anode would preclude its use (Abbas et al., 2022). Although the BDD electrode has great chemical stability, good electrocatalytic oxidation capacity, and a significant overpotential for oxygen evolution, its high cost and, particularly, the challenges of finding an adequate substrate for depositing the diamond layer limit its wide-scale implementation. SnO_2 electrodes, on the other hand, are considered preferable for the

oxidation of organic compounds with high OER and high activity. Due to its strong electrical conductivity and chemical stability, SnO_2 is recognized as a co-material for RuO_2 (Xu et al., 2015).

Several chemical deposition techniques have been used to create nanocrystalline SnO_2 thin films, including chemical vapor deposition, spray pyrolysis, sol-gel, and electrodeposition. Electrodeposition have been gained attention because of their benefits, including simplicity, cheap cost, low-temperature process, capacity to regulate characteristics and morphology by varied electrochemical factors, as well as deposition over vast and complicated regions (Daideche et al., 2017). Cathodic electrodeposition is an effective method for synthesizing nanocrystalline tin oxide. For the electrodeposition of metal oxides, OH ions or O radicals must be present on the electrode surface. Several kinds of oxygen sources are reported to be effective for the cathodic electrodeposition of oxides, including nitrate ions, hydrogen peroxide, and blown oxygen (Abdo et al., 2021).

The present work aimed to investigate the sonoelectrochemical process for organic pollutants removal from simulated wastewater over a SnO_2 electrode because several side reactions and the production of intermediates occurs when treating real refinery wastewater as well as the real wastewater with a variety of contaminants could take part in unknown reactions or serve as a catalyst to enhance unfavorable reactions. Phenol has been selected as a test compound, as it is one of the greatest challenging organic compounds to be treated by a sonoelectrochemical process, because oxidation of phenol changes it to large number of intermediates (other organic compounds) by sequence of reactions until the organic material entirely transformed to CO_2 and H_2O. The prepared electrodes were characterized, and the performance of the best anode electrode (obtained by the best deposition on it) was tested by organic removal using a sonoelectrochemical process.

EXPERIMENTAL WORK

Chemicals

All chemicals utilized in the present study were of reagent grade; thus, no further purification was required. These chemicals were $SnCl_2.2H_2O$ (with a purity of 97.0%, Thomas Baker), H_2SO_4 (with a purity of 98.0%, Alpha Chemika), phenol

(with a purity of 99.5%, LOBA Chemie), $NaNO_3$ (with a purity of 99.5%, Alpha Chemika), NaCl (with a purity of 99.9%, Central Drug House (P) Ltd-CDH), and HNO_3 (with a purity of 69-72%, Alpha Chemika). All aqueous solutions have been prepared by using distilled water.

Preparation of SnO_2 anode

Tin oxide electrodes were prepared by the cathodic electrodeposition method. Two graphite substrate plates of 6.5 cm*8 cm were firstly cleaned, polished by 2000-grit paper strips with water as a lubricant, and boiled in deionized water for 30 minutes. Then these substrates were electrochemically activated using CD of 14 mA/cm^2 at 90°C for 30 minutes in an electrolyte with 1.44 M of H_2SO_4. A hot plate magnetic stirrer (Nahita Blue, model 692/1) was used to maintain the electrolyte at the required temperature. The electrodes were washed using distilled water after the electrolysis. The cathodic deposition has been carried out with (25, 50, 75, and 100) mM $SnCl_2.2H_2O$, 100 mM $NaNO_3$ and (150, and 250) mM HNO_3 as shown in Table 1. The total volume of electrolytes was 500 ml. The solutions were stirred with 400 rpm at a temperature of 85 °C for 3 h to produce a stable solution (this is essential step for converting Sn^{2+} ions into Sn^{4+} ions).

A mercury thermometer was used to measure the contaminated solution temperature. After that, the prepared substrate was placed in the electrolytic solution with a 25 mm gap between the anode and cathode. The connection of electrodes to the power source (DC power supply, Maisheng, MS-605D) was attained by copper wires, the power supply was operated galvanostatically at 5 and 10 mA/cm^2, and the applied current was measured by the current multimeter. Throughout the experiment, the temperature of the electrolyte must be maintained at roughly 85°C. Cathodic deposition occurred for a certain period (1hr), after that, the electrode was washed with deionized water, dried at ambient temperature, and then calcined at 400°C for 4 hours.

Structural characterization

The physical structures of SnO_2 film were examined by X-ray diffraction using X-ray diffractometer (XRD 6000, SHIMADZU, Japan) powder diffractometer (CuKα radiation, λ= 1.5418 °A), surface morphology was characterized using scanning electron microscopy (SEM) (SEM TESCAN Vega III in College of Engineering/ Imir Kabir University/ Tehran) and chemical composition was analyzed using energy-dispersive X-ray spectroscopy (EDX) is attached with SEM

Sonoelectrochemical process

In the phenol removal experiments, a glass beaker containing a volume of 500 ml of simulated wastewater with 150 mg/l phenol concentrations was utilized. Figure 1 shows the electrochemical cell which was placed in a digital ultrasonic bath (Ultrasonic, model: 031S) at an ultrasonic frequency of 40 kHz (Zhang et al., 2020). Sonication was produced parallel to the liquid surface, and electrodes were fixed vertically in the solution. The prepared SnO_2 electrode was used as the anode and graphite as the cathode. The electrodes were connected to the DC power supply (MASHENG; MS-605D), and a constant CD was applied to the electrolytic cell for a specified time. Indirect oxidation was used in this study, so 3 g/l of NaCl (Divya et al., 2021) was added to the solution, several drops of H_2SO_4 were added to make the pH equal to 3, and the temperature of the electrolyte was maintained at about 25°C ± 2.

Electrode performance measurement

The performance of the SnO_2 anode sonoelectrochemical oxidation was investigated through

Table 1. Experiments of SnO_2 preparation

Electrode number	$SnCl_2.2H_2O$ concentration, mM	HNO_3 concentration, mM	Current density, mA/cm^2
1	25	150	5
2	25	150	10
3	25	250	10
4	50	250	10
5	75	250	10
6	100	250	10
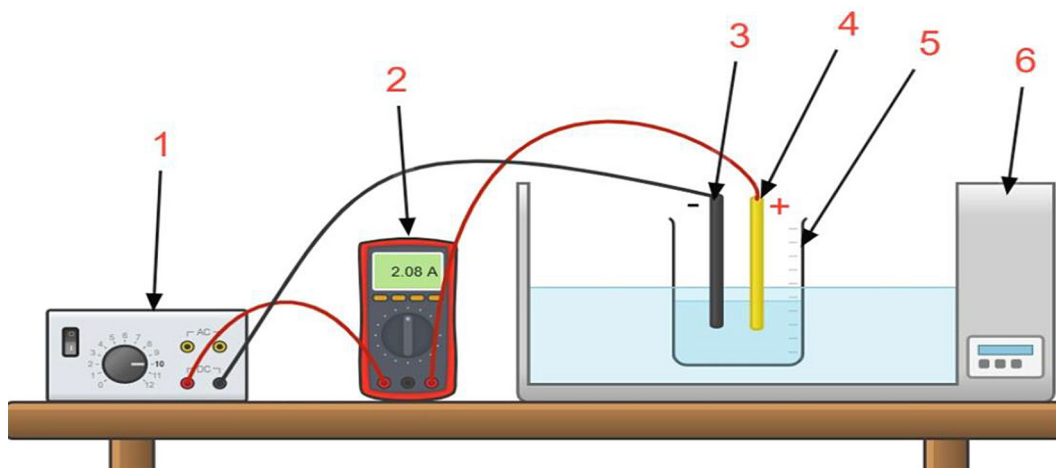
Figure 1. Schematic diagram of the sonoelectrochemical system, 1. power supply, 2. multimeter, 3. graphite cathode, 4. SnO₂ anode, 5. beaker containing the electrolyte, 6. digital ultrasonic bath

measurement of the phenol content and phenol can be converted into additional by product organic substances during oxidation, so it was better to estimate the chemical oxygen demand (COD). The phenol removal efficiency (PRE) is determined by Equation 1 (Hamad, 2021) :

$$PRE = \frac{IPC - CPC}{IPC} \times 100 \qquad (1)$$

where: IPC – the initial phenol concentration in (mg/l), CPC – the final phenol concentration in (mg/l).

The chemical oxygen demand evaluated with a COD reactor (Lovibond Water Testing, MD 200 COD, tube tests, Germany). The COD removal efficiency is determined by the Equation 2, as follows (Heydari Orojlou et al., 2022):

$$COD\ removal\% = \frac{CODi - CODt}{CODi} \times 100\% \qquad (2)$$

where: CODi and CODt – correspond to the initial and final COD concentration in (mg/l).

RESULTS AND DISCUSSION

The XRD results

Figure 2 shows the graphite XRD pattern prior to electrodeposition, which is exactly identical to the standard card and has a distinct sharp peak at 26 ° of 2θ. Figure 3 illustrates the XRD patterns of the deposit SnO₂ on graphite for different electrodes in the range (5–80) of 2θ. The average crystalline size of the deposit SnO₂ was calculated using Scherrer's equation (Khan et al., 2020).

$$D = (K*\lambda)/ (\beta*COS\ \theta) \qquad (3)$$

where: D – crystallite size (nm), k = 0.9 (Scherrer's constant), λ = 0.15406 nm (wavelength of the x-ray sources), β – diffraction line enlargement measured at a half maximum intensity in radians.

The results showed that electrodes number 4, 5, and 6 are the best electrodes for the electrodeposition process, where the peaks of tin oxide are evident and produce the smallest crystal size. It shows five peaks obtained at 2θ equal to 26.78° (110), 33.01° (101), 38.09° (200), 52.06° (211), and 54.23° (220) for electrode 4, 26.66° (110), 33.93° (101), 37.88° (200), 51.96° (211), and 54.18° (220) for electrode 5, and 26.56° (110), 33.96° (101), 38.14° (200), 51.99° (211), 54.38° (220) for electrode 6. Peak positions, relative intensity, and crystal size are shown in Table 2. These peaks are all in strong agreement with the data provided for tetragonal SnO₂ (JCPDS no. 41-1445) and previous studies (Daideche et al., 2017 b).

It was found that the crystal size of the SnO₂ deposit was determined to be 16.03 and 19.76 nm for 5 and 10 mA/cm² of applied current density, respectively; this means that the crystal size increases as the applied current density increases, a result that was supported by other studies (Salman et al., 2019), the crystal size for the two HNO₃ concentrations (150 and 250 mM) was 19.76 and 5.33 nm, respectively, so the crystal size decreases as the concentration of HNO₃ increases, and The crystal size was changed slightly from 3.79 to 5.43 nm when the SnCl₂.2H₂O concentration increased from 25 to 100 Mm.
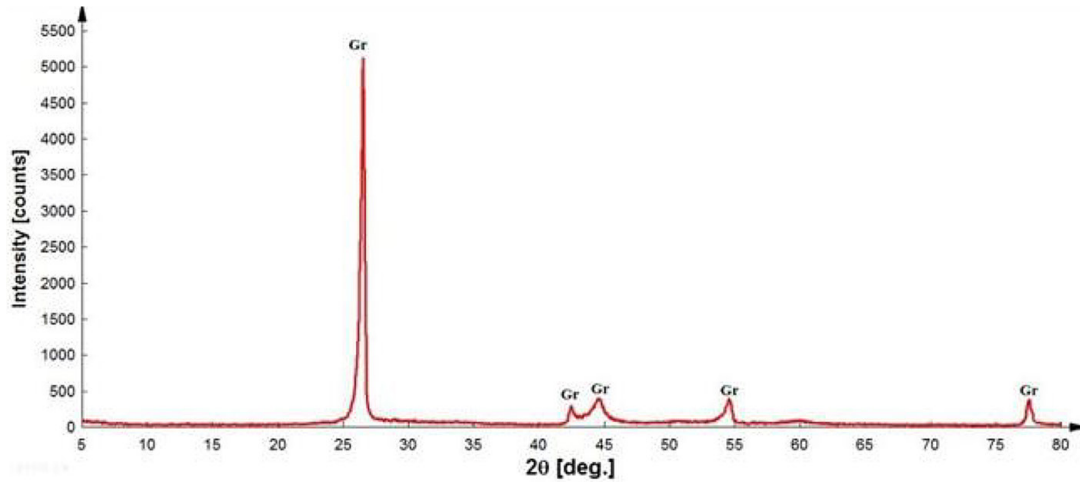
Figure 2. Graphite XRD pattern prior to electrodeposition
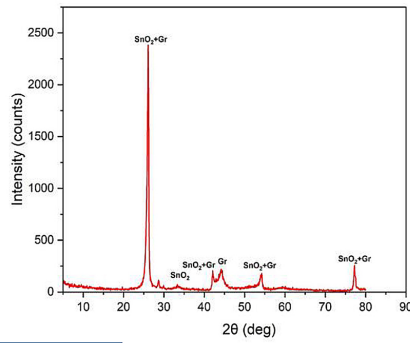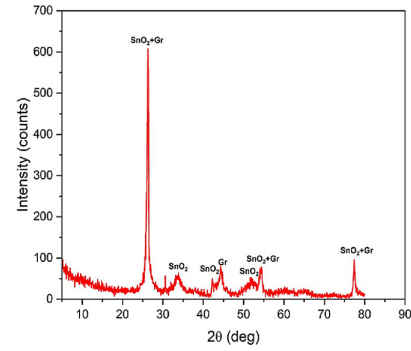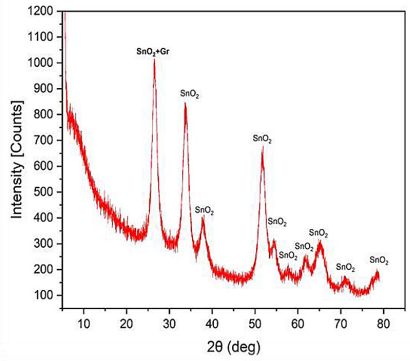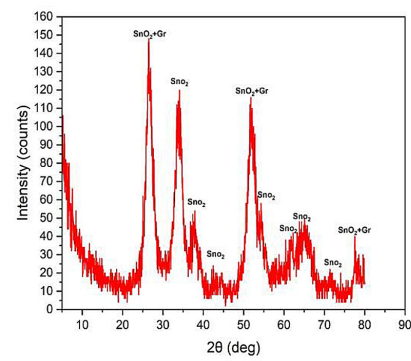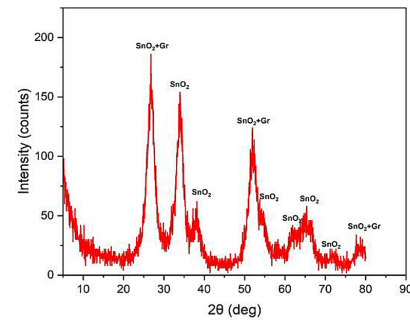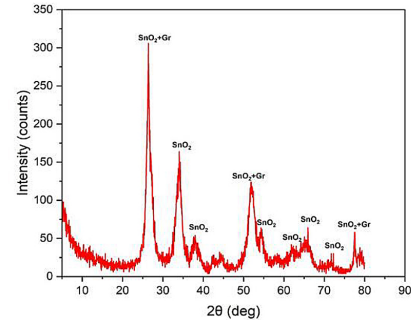
Figure 3. XRD of SnO$_2$ electrode

Table 2. Data analysis from XRD patterns in Figure 3

Electrode number	Peak positions					Relative intensity					Crystal size (nm)
	110	101	200	211	220	110	101	200	211	220	
JCPDS no. (41-1445)	26.61	33.89	37.95	51.78	54.75	100	75	21	57	14	—
1. (25 mM $SnCl_2.2H_2O$, 150 mM HNO_3, and CD=5 mA/cm²)	26.21	—	—	—	54.24	100	—	—	—	8	16.03
2. 25 mM $SnCl_2.2H_2O$, 150 mM HNO_3, and CD =10 mA/cm²	26.29	33.49	—	—	54.43	100	5	—	—	9	19.76
3. (25 mM $SnCl_2.2H_2O$, 250 mM HNO_3, and CD =10 mA/cm²)	26.55	33.89	37.99	51.70	54.34	100	61.05	15.59	52.06	11.50	5.33
4. (50 mM $SnCl_2.2H_2O$, 250 mM HNO_3, and CD =10 mA/cm²)	26.78	34.01	38.09	52.06	54.23	100	83	20	63	24	3.79
5. (75 mM $SnCl_2.2H_2O$, 250 mM HNO_3, and CD =10 mA/cm²)	26.66	33.93	37.88	51.96	54.18	100	73	24	76	27	3.96
6. (100 mM $SnCl_2.2H_2O$, 250 mM HNO_3, and CD =10 mA/cm²)	26.56	33.96	38.14	51.99	54.38	100	53	12	43	18	5.43

The SEM and EDX results

The effect of the current density

The applied current density has a significant effect on the surface morphology of SnO_2 deposits. It seems that when the CD increases, the crystal size will enlarge with greater crystallinity (Raj et al., 2015). This effect is explained by the metallic ions diffusing to the substrate more quickly than usual and quick nucleation takes place during the electrodeposition process, as illustrated in Figure 4 (Arote et al., 2015; Salman et al., 2019). EDX has been employed to detect the composition of the electrode elements. The EDX results indicated the presence of Sn and oxygen elements, which indicates that the SnO_2 was deposited successfully on the electrode surface. Table 3 shows that when the CD is 5 mA/Cm² (electrode number 1(, the weight percentage of Sn is 7.78 and oxygen is 20.59, while when the CD increases to 10 mA/Cm² (electrode number 2(, the weight percentage of Sn is 34.21 and oxygen is 18.30., this demonstrated that the deposition efficiency

of SnO_2 increases along with CD, because more (Sn^+) and (OH^-) ions (building blocks of film production) accumulated towards the cathode surface when increasing CD (Hessam et al., 2022).

The effect of HNO_3 concentration

It is well known that hydroxyl ions (OH^-) or O radicals must be present close to the electrode surface in order to prepare metal oxide by electrodeposition (Abdo et al., 2021). Nitric acid was used as the source of oxygen in this work, and tin chloride dehydrate ($SnCl_2.2H_2O$) served as the Sn^{2+} source and the prior treatment of the electrolyte is essential for converting Sn^{2+} ions into Sn^{4+} ions. The half-reaction of the cathode electrode surface is depicted below, as follows (Daideche et al., 2017): The deposition of the SnO_2 electrode was considered to involve the formation of OH^- ions on the electrode surface, as shown in Equation 4.

$$NO_3^- + H_2O + 2e^- \rightarrow NO^{2-} + 2OH^- \qquad (4)$$

The stannic ions from the bulk solution reacted with the OH^- ions that had formed on the
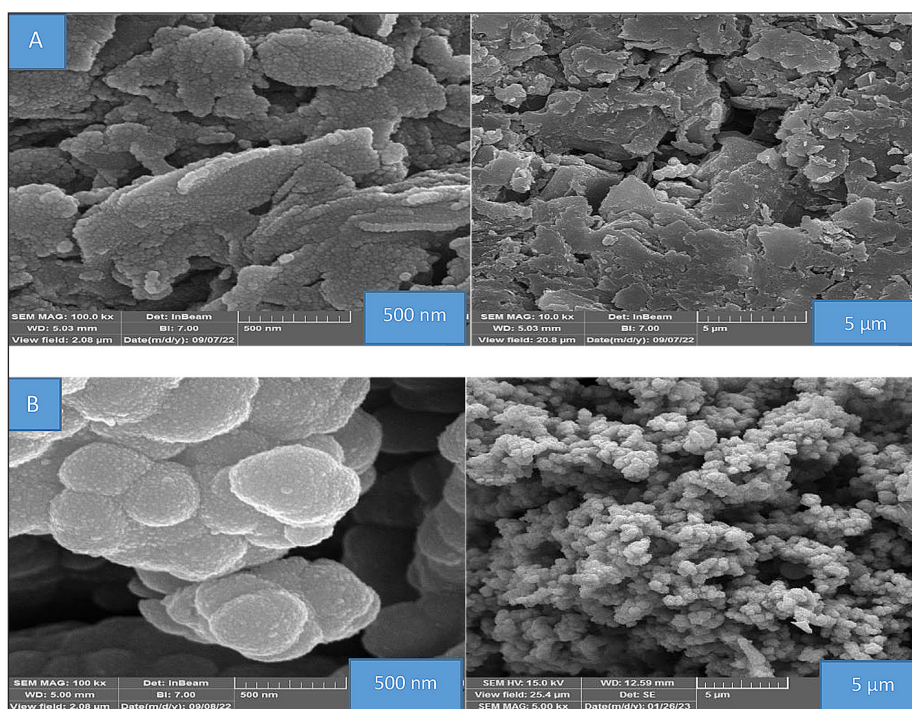
Figure 4. SEM of SnO$_2$ electrode at (A) CD =5 mA/cm^2, (B) CD =10mA/cm^2, 25 mM SnCl$_2$.2H$_2$O, time= 1 hr, and 150 mM HNO$_3$

Table 3. EDX of SnO$_2$ electrode at (A) CD =5mA/cm^2, (B) CD =10mA/cm^2, 25 mM SnCl$_2$.2H$_2$O, time= 1 hr, and 150 mM HNO$_3$

Element	Electrode 1 (A: 5 mA/cm^2)		Electrode 2 (B: 10 mA/cm^2)	
	Weight, %	Atomic, %	Weight, %	Atomic, %
C	34.51	56.04	9.08	23.14
O	20.59	25.11	18.30	34.99
Sn	7.78	1.28	34.21	8.82
Si	2.19	1.52	3.90	4.25
S	15.51	9.43	21.61	20.62
Ca	10.92	5.31	5.27	4.02
Ag	0.00	0.00	2.34	0.66
Cl	0.00	0.00	3.58	3.09
I	8.50	1.31	1.71	0.41
Total	100.00	100.00	100.00	100.00

electrode surface to create nanocrystalline SnO$_2$, as shown in Equation 5.

$$Sn^{4+} + 4OH^- \rightarrow SnO_2 + 2H_2O \qquad (5)$$
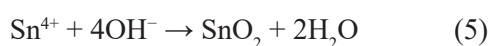
However, because of the system complexity, the next two reduction processes could coexist and lead to the deposition of Sn metal, as illustrated in Equations 6 and 7.

$$Sn^{4+} + 2e^- \rightarrow Sn^{2+} \qquad (6)$$

$$Sn^{2+} + 2e^- \rightarrow Sn \qquad (7)$$
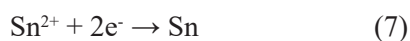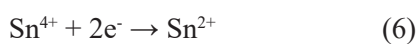
As a result, the deposition potential of reaction (4) shifts in the positive direction with an increase in NO$_3$ concentration and electrolyte acidity, whereas reaction (6) shifts in the opposite direction with a decrease in Sn^{4+} concentration. Hence, the favored deposition of SnO$_2$ occurs whenever the ratio of [HNO$_3$] to [Sn^{4+}] is high (Chen et al., 2010, 2017).

Figure 5 shows the SEM morphology of SnO$_2$ electrodes. It appears that the crystal size increases along with the HNO$_3$ concentration

increases, , and it can be seen that small particles have been agglomerated and have the same spherical morphology as well as porous surface, which leads to a large surface area at different HNO_3 concentrations.

EDX results (Table 4) showed that when the concentration of HNO_3 is 150 mM (electrode number 2(, the weight percentage of Sn is 34.21 and oxygen is 18.03, while when the concentration of HNO_3 is 250 mM (electrode number 3(, the weight present of Sn is 33.94 and oxygen is 24.63. This demonstrated that the

deposit phases changed from Sn and SnO_2 to pure SnO_2 with the increase in HNO_3 concentration (Chen et al., 2010).

The effect of SnCl$_2$.2H$_2$O concentration

Figure 6 shows the SEM pictures, which demonstrate the dramatic impact of the $SnCl_2.2H_2O$ concentration on the shape of the deposited film. Over the whole surface of the graphite substrate, irregular spherical granules can be seen. Large crystallites are created as the nanocrystals
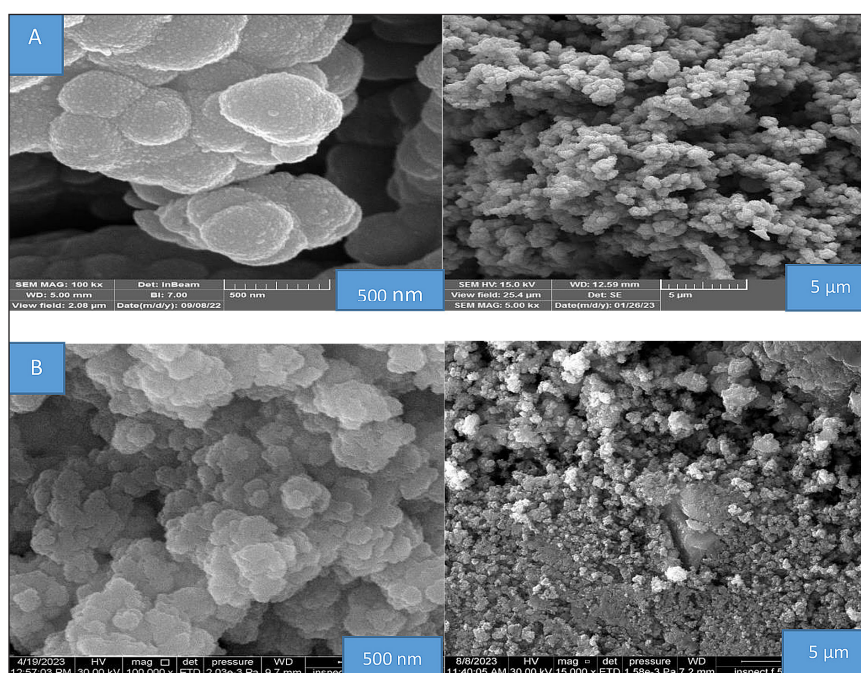
Figure 5. SEM of SnO_2 electrode at (A) 150 mM HNO_3, (B) 250 mM HNO_3, CD =10 mA/cm^2, time=1hr, and 25 mM $SnCl_2.2H_2O$

Table 4. EDX of SnO_2 electrode at (A) 150 mM HNO_3, (B) 250 mM HNO_3, CD =10 mA/cm^2, time=1hr, and 25 mM $SnCl_2.2H_2O$

Element	Electrode 2 (A: 150 mM HNO_3)		Electrode 3 (B: 250 mM HNO_3)	
	Weight, %	Atomic, %	Weight,%	Atomic, %
C	9.08	23.14	9.64	27.33
O	18.30	34.99	25.38	54.02
Sn	34.21	8.82	64.99	18.65
S	21.61	20.62	_	_
Cl	3.58	3.09	_	_
Ca	5.27	4.02	_	_
Ag	2.34	0.66	_	_
Si	3.90	4.25	_	_
I	1.71	0.41	_	_
Total	100.00	100.00	100.00	100.00

aggregated. A crystallite like this is organized in a haphazard, non-uniform manner to create a porous morphology (Santos et al., 2014).

It can be seen from Figure 6 b that some agglomerated deposits were obtained at a concentration of $SnCl_2.2H_2O$ equal to 50 mM (electrode number 4(and illustrate a huge interconnected, uniform porous structure formed by the unevenly linked nanoparticles. No cracks appeared, but these cracks were observed at higher concentrations. When the salt concentration was 75 and 100 mM (electrode number 5 and 6) the surface covering with SnO_2 was homogeneous and excellent, but the electrode surface was distinguished by a "cracked-mud" morph. In line with this theory, through electrodeposition, it is more likely to produce pure SnO_2 with a lower concentration of $SnCl_2.2H_2O$. However, the deposition rate can be too sluggish if the $SnCl_2.2H_2O$ concentration is too low (25 mM (electrode number 3)). Therefore, the deposition rate was excellent at 50 mM SnCl2. 2H2O salt concentration, and 250 mM HNO3 concentration. This is confirmed by the results of the EDX, as in Table 5 (Chen et al., 2010).

Phenol and COD removal

With sonoelectro-oxidizing phenol (150 mg/l) in the presence of 3 g/l NaCl and several drops of H_2SO_4 as a supporting electrolyte, 25 mA/cm^2 CD, and 40 kHz ultrasonic frequency, the performance of the best-produced SnO_2 electrodes numbers 4,
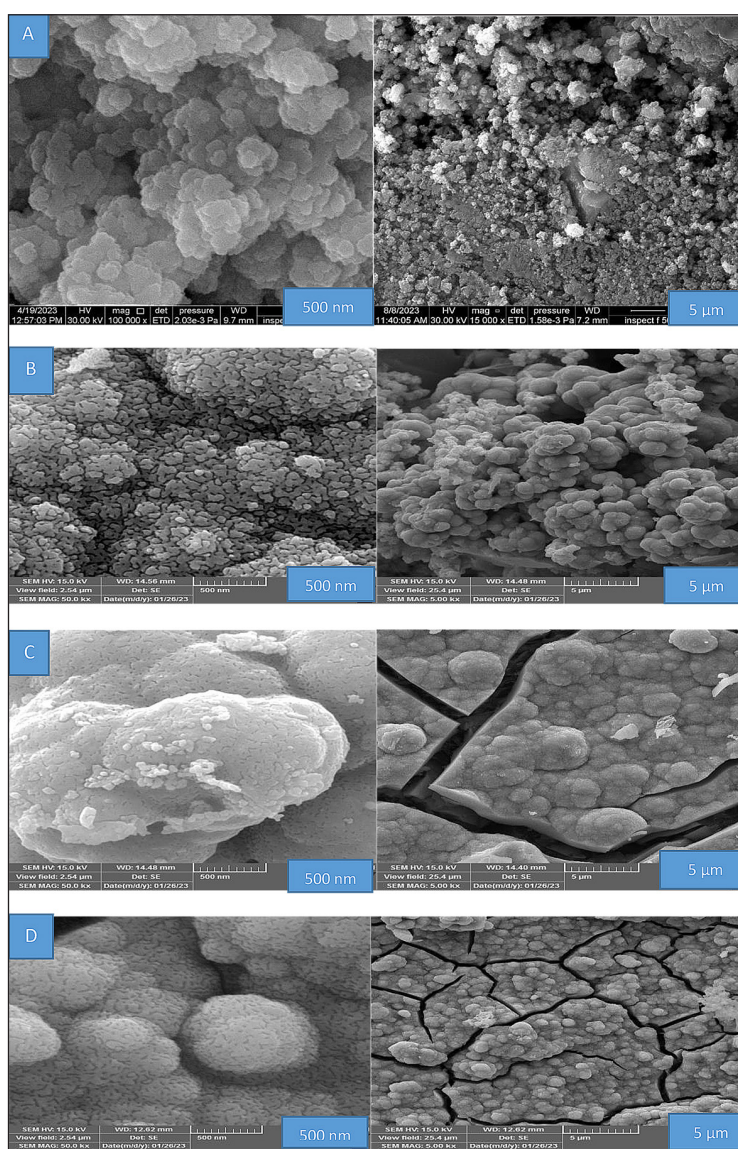
Figure 6. SEM of SnO_2 electrode at (A) 25 mM $SnCl_2.2H_2O$, (B) 50 mM $SnCl_2.2H_2O$ (C) 75 mM $SnCl_2.2H_2O$, (D) 100 mM $SnCl_2.2H_2O$, CD =10 mA/cm^2, time= 1hr, and 250 mM HNO$_3$

Table 5. EDX o of SnO$_2$ electrode at (A) 25 mM SnCl$_2$.2H$_2$O, (B) 50 mM SnCl$_2$.2H$_2$O (C) 75 mM SnCl$_2$.2H$_2$O, (D) 100 mM SnCl$_2$.2H$_2$O, CD =10 mA/cm^2, time= 1hr, and 250 mM HNO$_3$

Element	Electrode 3 (A: 25 mM SnCl$_2$·2H$_2$O)		Electrode 4 (B: 50 mM SnCl$_2$·2H$_2$O)		Electrode 5 (C: 75 mM SnCl$_2$·2H$_2$O)		Electrode 6 (D: 100 mM SnCl$_2$·2H$_2$O)	
	Weight, %	Atomic, %	Weight, %	Atomic, %	Weight,%	Atomic, %	Weight, %	Atomic, %
C	9.64	27.33	5.72	17.39	5.4	17.3	2.00	7.93
O	25.38	54.02	27.14	61.95	25.2	60.3	20.50	61.00
Sn	64.99	18.65	67.14	20.66	69.3	22.3	77.50	31.08
Total	100.00	100.00	100.00	100.00	100.00	100.00	100.00	100.00

5, and 6 (have the best structural characteristics) was investigated. Figure 7 demonstrates that the phenol removal was 76.87, 72.34, and 66.23 for 4, 5, and 6 electrodes, respectively, and Figure 8 shows that the COD removal was 69.68, 63.56, and 58.73 for 4, 5, and 6 electrodes, respectively. This investigation found that electrode number 4 (50 mM SnCl$_2$.2H$_2$O, CD =10 mA/cm^2, and 250 mM HNO$_3$) gave the best phenol and COD removal, and it can be said that the favored deposition of SnO$_2$ occurs whenever the ratio of [HNO$_3$] to [Sn^{4+}] is high (Chen et al., 2010), so the SnCl$_2$.2H$_2$O concentration in this investigation was set at 50 mM and the HNO$_3$ concentration was set at 250 mM. In electrode number 4 for the SEM test, crystals were appeared as homogeneous and there were no cracks, but in electrodes 5 and 6, cracks appeared in the SEM test, and the phenol removal was lesser. This may be due to the presence of cracks that make the surface breakable and quick to separate from the electrode at the start of the process. Electrode number

4 demonstrated the maximum removal efficiency. This is further supported by the characterization testing at rest, allowing it to be employed in the subsequent removal processes.

To compare their impact on phenol removal from wastewater, sonoelectrochemical oxidation of phenol using NaCl and Na$_2$SO$_4$ as the electrolytes was carried out in two distinct reactors at 25 mA/cm^2 CD, 40 kHz ultrasonic frequency, 150 mg/l phenol concentration, and at 25°C. Figure 9 shows the phenol removal by using the different employed electrolyte. The 76.87% degradation of phenol was achieved when using NaCl as the electrolyte. However, 64.68% of the phenol was removed when using Na$_2$SO$_4$. Figure 10 shows the COD removal efficiency was 69.68% during using NaCl as an electrolyte. However, 51.87% COD was removed when using Na$_2$SO$_4$. It is evident that NaCl as an electrolyte is more effective in the degradation of phenol because, in the wastewaters containing NaCl, active chloro-species like chlorine, hypochlorite, and
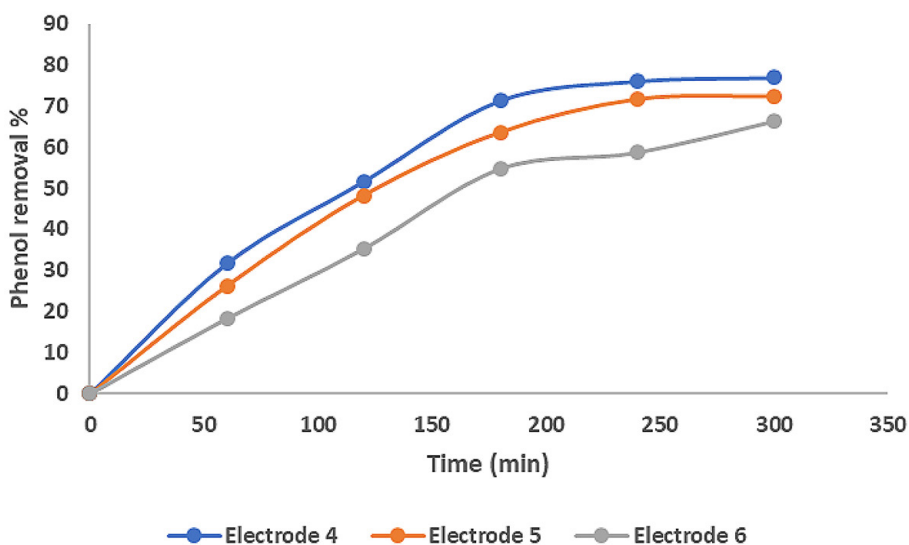
Figure 7. Phenol removal at different electrodes, CD = 25 mA/cm^2, temp. = 25 °C, NaCl conc.= 3 g/l, pH = 3 and 40 kHz ultrasonic frequency
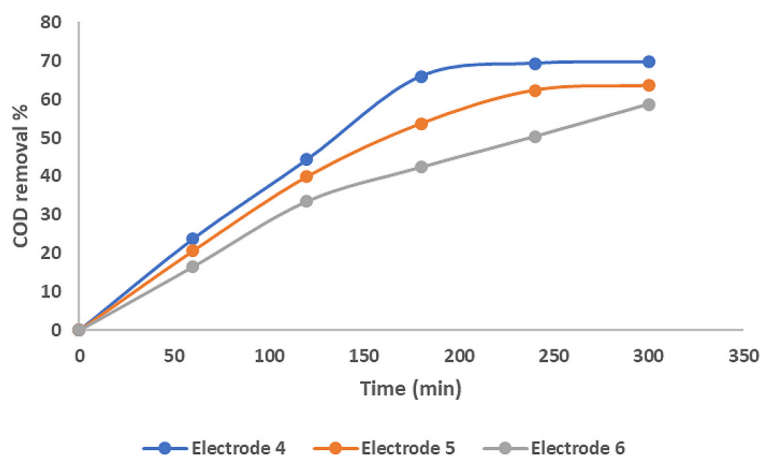
Figure 8. COD removal at different electrodes, CD = 25 mA/cm², temp. = 25 °C, NaCl conc. = 3 g/l, pH = 3 and 40 kHz ultrasonic frequency

hypochlorous acid are generated at the anode and consequently oxidize the pollutants. In most circumstances, the presence of an appropriate chloride concentration can remove both inorganic and organic contaminants. An improvement in removal effectiveness was produced by the inclusion of chloride ions of the electrolyte (Divya et al., 2021). In turn, when using Na_2SO_4 as the electrolytes, peroxodisulfate ($S_2O_8^{-2}$) is produced under thermally boosted conditions (temperature 30-100°C), $S_2O_8^{-2}$ can be transformed to obtain activated persulfate, and this generates sulfate-free radicals that can remove organic pollutants like phenol. In this investigation, the temperature in the reactors reached about 30°C, but this condition was insufficient to generate the theoretical

amount of sulfate free radicals (Zambrano et al., 2019). Previous investigations have shown that CD is an important factor of the electrochemical process. Higher CD is beneficial to the combined system (Ang et al., 2022). The sonoelectrochemical procedure took place at various CD (10, 25, 40) mA/cm², a pH of 4, an ultrasonic frequency of 40 kHz, a temperature of 25°C, and 3 g/l of NaCl. The findings of phenol concentration were recorded for up to 5 hours and plotted in Figure 11. The phenol removal percentage increased from 62.94 to 76.87 and 100%. As the CD increases from 10 to 25 and 40 mA/cm², respectively, Figure 12 shows that the COD removal percentages were 45.57, 69.68, and 100% at 10, 25, and 40 mA/cm², respectively, after 5h of electrolysis. This indicates that the increase
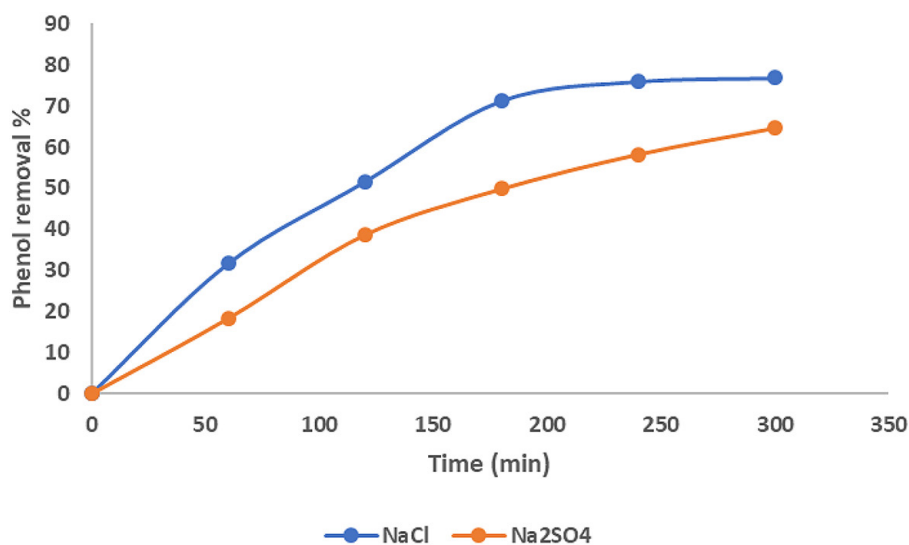
Figure 9. The effect of the type of electrolyte e on phenol removal at CD= 25 mA/cm², temp. = 25°C, NaCl conc. = 3 g/l, pH = 3 and 40 kHz ultrasonic frequency
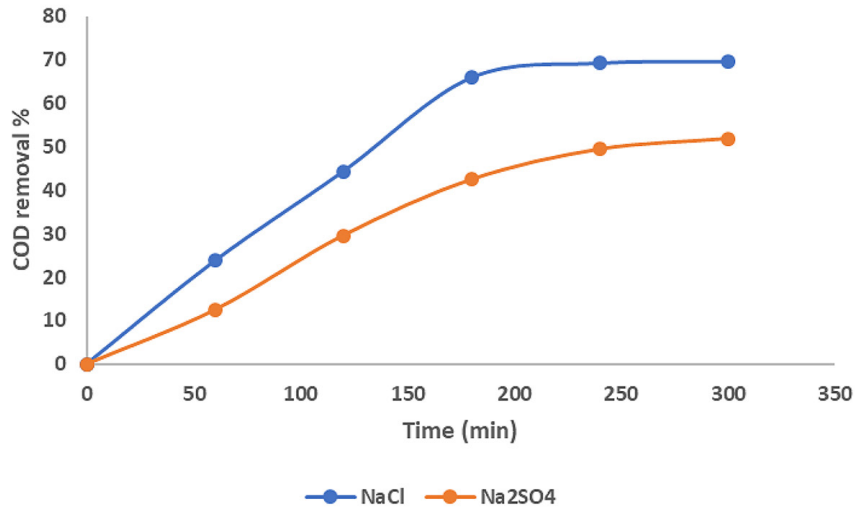
Figure 10. The effect of the type of electrolyte on COD removal at CD = 25 mA/cm^2, temp. = 25°C, NaCl conc.= 3 g/l, pH= 3 and 40 kHz ultrasonic frequency
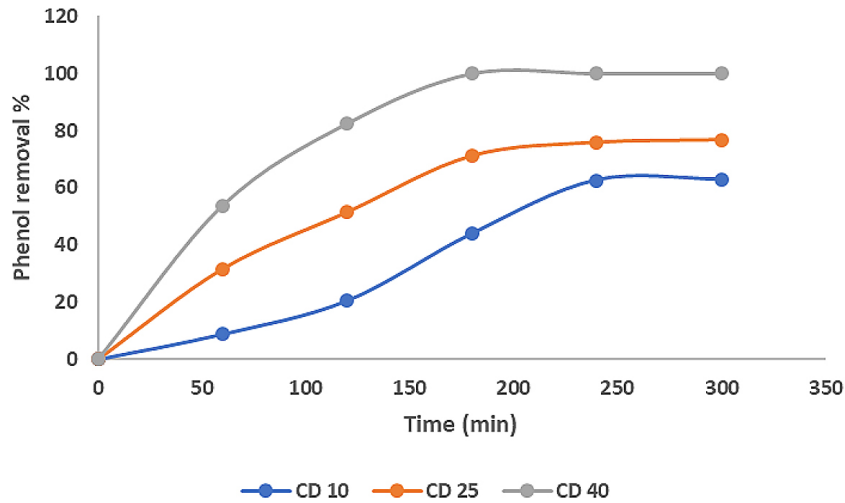
Figure 11. The effect of CD on phenol removal, temp. = 25°C, NaCl conc.= 3 g/l, pH = 3 and 40 kHz ultrasonic frequency
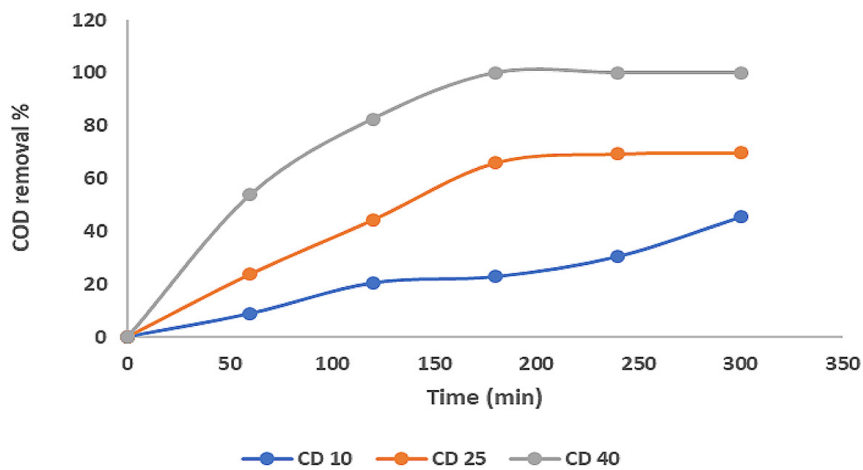
Figure 12. The effect of CD on COD removal, temp. = 25°C, NaCl = 3 g/l, pH = 3 and 40 kHz ultrasonic frequency

in CD caused enhancement in phenol degradation, and this occurs because there is now more electrochemically produced hydrogen peroxide as a result of the electrolysis, and when the concentration of hydrogen peroxide rises, hydroxyl radical ($OH^{\cdot}$) rises to a level sufficient to react with the organic pollutants already present in the treated solution, reducing the concentration of phenol. The obtained findings concur with those of other studies (Abbas et al., 2016, 2021; Ahmed et al., 2023).

CONCLUSIONS

Successful preparation and testing of a SnO_2 electrode by cathodic electrodeposition for the process of phenol degradation were attained in the present study. According to the XRD data, tetragonal SnO_2 is the significant phase structure at all deposits. It was found that the applied current density, HNO_3 concentration, and $SnCl_2.2H_2O$ concentration were essential for preventing the co-deposition of Sn and had a significant impact on the morphology of the deposits. These processing parameters could be precisely controlled to produce dense SnO_2 films that adhered well to the graphite substrate. The electrode which prepared at 10 mA/cm$_2$, 50 mM of $SnCl_2.2H_2O$, and 250 mM of HNO_3 is the best electrode which produced the smallest crystal size, with no cracks, and gave the best phenol and other organic by products removal. Therefore, the current electrode is a promising method for sonoelectrochemical indirect oxidation to remove a variety of organic contaminants from wastewater. The combined sonochemical and electrochemical treatments combined display an advantageous effect. Using sodium chloride as the electrolyte leads to a higher degradation of phenol compared with sodium sulfate. The performance of the sonoelectrochemical removal of organic compounds is most affected by CD. The phenol and COD removal efficiency reached 100% at current density of 40 mA/cm^2 at temp. = 25°C, NaCl conc.= 3 g/l, pH = 3 and 40 kHz ultrasonic frequency. The results of current research showed that the SnO_2 electrode is very promising in the removal of organics by sonoelectrochemical oxidation.

REFERENCES

1. Abbas A.S., Hafiz M.H., Salman R.H., 2016. Indirect electrochemical oxidation of phenol using rotating cylinder reactor. Iraqi Journal of Chemical and Petroleum Engineering., 17, 43–55.

2. Abbas R.N., Abbas A.S., 2022. Kinetics and energetic parameters study of phenol removal from aqueous solution by electro-fenton advanced oxidation using modified electrodes with PbO2 and graphene. Iraqi Journal of Chemical and Petroleum Engineering., 23, 1–8.

3. Abbas Z.I., Abbas A.S., 2021. Optimization of the electro-fenton process for cod reduction from refinery wastewater. Environmental Engineering and Management Journal., 19, 2029–2037.

4. Abdo H.S., Sarkar A., Gupta M., Sahoo S., Mohammed J.A., Ragab S.A., Seikh A.H., 2021. Low-cost high-performance sno2–cu electrodes for use in direct ethanol fuel cells. Crystals., 11, 1–12.

5. Ahmed Y.A., Salman R.H., 2023. Simultaneous electrodeposition of multicomponent of Mn–Co–Ni oxides electrodes for phenol removal by anodic oxidation. Case Studies in Chemical and Environmental Engineering., 8.

6. Al-Alawy A.F., Al-Ameri M K., 2017. Treatment of simulated oily wastewater by ultrafiltration and nanofiltration processes. Iraqi Journal of Chemical and Petroleum Engineering., 18, 71–85.

7. Al-Jandeel H.A.K., 2013. Removal of phenolic compounds from aqueous solution by using agricultural waste (Al-Khriet). Iraqi Journal of Chemical and Petroleum Engineering., 14, 55–62.

8. Al-Obaidy A., 2013. Removal of phenol compounds from aqueous solution using coated sand filter media. Iraqi Journal of Chemical and Petroleum Engineering., 14, 23–31.

9. Ang W.L., McHugh P.J., Symes M.D., 2022. Sonoelectrochemical processes for the degradation of persistent organic pollutants. Chemical Engineering Journal., 444.

10. Arote S.A., Tabhane V., Gunjal S.D., Mohite K.C., Pathan H., 2015. Structural and optical properties of electrodeposited porous SnO2 films: Effect of applied potential and post deposition annealing treatment. Macromolecular Symposia. Wiley-VCH Verlag, Vol. 347pp. 75–80.

11. Chen J.Y., Chueh C.C., Zhu Z., Chen W.C., Jen A.K.Y., 2017. Low-temperature electrodeposited crystalline SnO2 as an efficient electron-transporting layer for conventional perovskite solar cells. Solar Energy Materials and Solar Cells., 164, 47–55.

12. Chen X., Liang J., Zhou Z., Duan H., Li B., Yang Q., 2010. The preparation of SnO2 film by electrodeposition. Materials Research Bulletin., 45, 2006–2011.

13. Daideche K., Azizi A., 2017a. Electrodeposition of tin oxide thin film from nitric acid solution: The role of pH. Journal of Materials Science: Materials in Electronics., 28, 8051–8060.

14. Daideche K., Azizi A., 2017b. Electrodeposition of

tin oxide thin film from nitric acid solution: The role of pH. Journal of Materials Science: Materials in Electronics., 28, 8051–8060.

15. Daideche K., Azizi A., 2017c. Electrodeposition of tin oxide thin film from nitric acid solution: The role of pH. Journal of Materials Science: Materials in Electronics., 28, 8051–8060.

16. Divya N., Sreerag A.V, Yadukrishna J.T., Soloman P.A., 2021. A study on electrochemical oxidationof phenol for wastewater remediation. IOP Conference Series: Materials Science and Engineering. IOP Publishing, Vol. 1114.

17. Fajri N.R., Mohammed R.N., 2023. Removal of organic pollutants from wastewater using different oxidation strategies. Journal of Ecological Engineering., 24, 351–359.

18. Hamad H.T., 2021. Removal of phenol and inorganic metals from wastewater using activated ceramic. Journal of King Saud University - Engineering Sciences., 33, 221–226.

19. Hessam R., Najafisayar P., Rasouli S.S., 2022. A comparison between growth of direct and pulse current electrodeposited crystalline SnO2 films; electrochemical properties for application in lithium-ion batteries. Materials for Renewable and Sustainable Energy., 11, 259–266.

20. Heydari Orojlou S., Rastegarzadeh S., Zargar B., 2022. Experimental and modeling analyses of COD removal from industrial wastewater using the TiO2–chitosan nanocomposites. Scientific Reports., 12.

21. Kassob A.N., Abbar A.H., 2022. Treatment of petroleum refinery wastewater by graphite–graphite electro fenton system using batch recirculation electrochemical reactor. Journal of Ecological Engineering., 23, 291–303.

22. Khan H., Yerramilli A.S., D'Oliveira A., Alford T.L., Boffito D.C., Patience G.S., 2020, June 1. Experimental methods in chemical engineering: X-ray diffraction spectroscopy—XRD. Canadian Journal of Chemical Engineering.

23. Majeed N.S., 2017. Inverse fluidized bed for chromium ions removal from wastewater and produced water using peanut shells as adsorbent. 2017 International Conference on Environmental Impacts of the Oil and Gas Industries: Kurdistan Region of Iraq as a Case Study (EIOGI), Koya-Erbil, Iraq., 9–14.

24. Mezaal D.K., 2019. Removal Of Parachlorophenol From Synthetic Waste Water Using Advanced Electrochemical Oxidation Process (M.Sc. Thesis). Al-Nahrain University, Baghdad.

25. Naser G.F., Mohammed T.J., Abbar A.H., 2021. Treatment of Al-Muthanna petroleum refinery wastewater by electrocoagulation using a tubular batch electrochemical reactor. IOP Conference Series: Earth and Environmental Science. IOP Publishing Ltd, Vol. 779.

26. Raj D.V., Ponpandian N., Mangalaraj D., Viswanathan C., 2015. Electrodeposition of macroporous SnO2 thin films and its electrochemical applications. Materials Focus., 4, 245–251.

27. Salman R.H., Hafiz M.H., Abbas A.S., 2019. Preparation and characterization of graphite substrate manganese dioxide electrode for indirect electrochemical removal of phenol. Russian Journal of Electrochemistry., 55, 407–418.

28. Santos D., Lopes A., Pacheco M.J., Gomes A., Ciríaco L., 2014. The oxygen evolution reaction at Sn-Sb oxide anodes: Influence of the oxide preparation mode. Journal of The Electrochemical Society., 161, H564–H572.

29. Thokchom B., Pandit A.B., Qiu P., Park B., Choi J., Khim J., 2015. A review on sonoelectrochemical technology as an upcoming alternative for pollutant degradation. Ultrasonics Sonochemistry., 27, 210–234.

30. Thwaini H.H., Salman R.H., 2023. Modification of electro-fenton process with granular activated carbon for phenol degradation – optimization by response surface methodology. Journal of Ecological Engineering., 24, 92–104.

31. Xu L., Li M., Xu W., 2015. Preparation and characterization of Ti/SnO2-Sb electrode with copper nanorods for AR 73 removal. Electrochimica Acta., 166, 64–72.

32. Zambrano J., Min B., 2019. Comparison on efficiency of electrochemical phenol oxidation in two different supporting electrolytes (NaCl and Na2SO4) using Pt/Ti electrode. Environmental Technology and Innovation., 15.

33. Zhang M., Zhang Z., Liu S., Peng Y., Chen J., Yoo Ki S., 2020. Ultrasound-assisted electrochemical treatment for phenolic wastewater. Ultrasonics Sonochemistry., 65.

34. Zhao W., Xing J., Chen D., Bai Z., Xia Y., 2015. Study on the performance of an improved Ti/SnO2-Sb2O3/PbO2 based on porous titanium substrate compared with planar titanium substrate. RSC Advances., 5, 26530–26539.